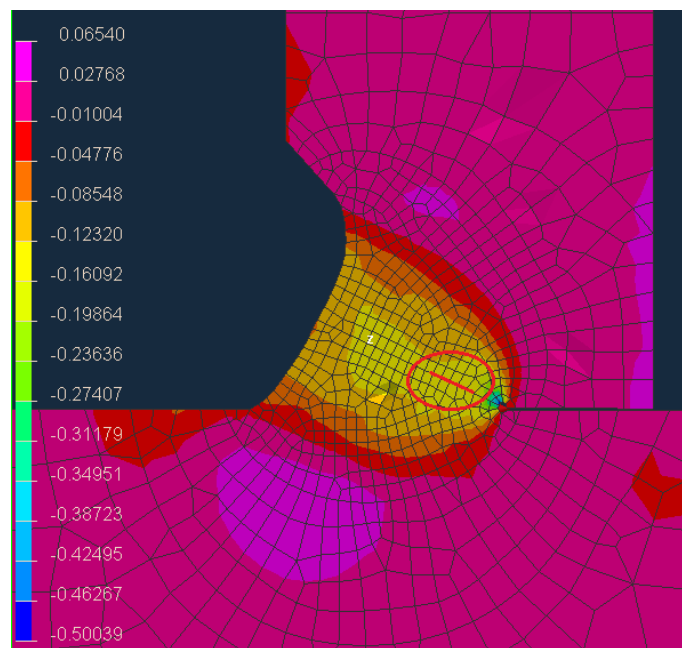


PREDCRACK

Predictive model of risk for hot cracks in high strength steel



Författare: David Löveborn, Paul Janiak
Datum: 2017-06-27
Projekt inom: Hållbar produktion

FFI Fordonsstrategisk
Forskning och
Innovation

VINNOVA

Energimyndigheten

TRAFIKVERKET

FKG

VOLVO

SCANIA

VOLVO

Innehållsförteckning

1 Sammanfattning	3
2 Executive summary in English.....	3
3 Introduction	4
4 Background	4
4.1 Physical experiments from earlier study	4
4.2 Materials.....	8
5 Method.....	8
5.1 Thermodynamic calculations.....	8
5.2 Analysis of welded material and crack surfaces	9
5.3 FE-simulations.....	9
6 Results	9
6.1 Thermodynamic calculations.....	9
6.2 Analysis of welded material and crack surfaces	12
6.3 FE-simulations.....	14
6.3.1 2D-simulation.....	14
6.3.2 3D-simulations – cases from previous project.....	16
6.3.3 3D-simulations – industrial cases.....	20
7 Spridning och publicering	27
7.1 Kunskaps- och resultatspridning.....	27
7.2 Publikationer.....	27
8 Discussion	27
9 Conclusions.....	28
10 Future work.....	28
11 Deltagande parter och kontaktpersoner.....	29
12 References	29

1 Sammanfattning

Denna förstudie har syftat till att utvärdera möjligheten att använda FE-simuleringar som ett verktyg för prediktering av risken för varmsprickor i svetsar i höghållfasta stål. Att undvika varmsprickor är ett krav för att uppnå god utmattningshållfasthet i MAG-svetsade konstruktioner. Orsaken till varmsprickor är idag inte fullt utredd och dagens riktlinjer och verktyg klarar inte av att prediktera risken för varmsprickor fullt ut. Risken att varmsprickorna är icke-ytbrytande är stor, vilket medför att de endast kan detekteras med hjälp av volymetriska OFP-metoder, så som röntgen- och ultraljudstestning. I värsta fall upptäcks inte sprickorna förrän i utmattningsbrott i komponenter som är i användning.

Detta projekt är baserat på ett tidigare projekt hos Swerea KIMAB, där inverkan av grund- och tillsatsmaterial, samt spaltbredd i T-fogar utvärderats med avseende på varmsprickrisk. Den största delen av simuleringarna i detta projekt har utgått ifrån prover framtagna i det tidigare projektet.

Målet med denna förstudie var att utvärdera och utveckla en metodik och en prediktiv modell som skulle kunna användas som riktlinjer för minimering av varmsprickrisken i MAG-svetsade T-förband. Modellen har verifierats mot både prover framtagna i det tidigare projektet och mot problematiska industrifall.

Resultaten från projektet visar att FE-simuleringar skulle kunna användas för att jämföra varmsprickrisken mellan olika förband och fogprepareringar. Resultaten från simuleringarna visar på en korrelation mellan töjningarna i svetsen under stelningsförloppet och risken för varmsprickor. De undersökta töjningarna ligger i det mest påkända området och går transversellt mot sprickriktningen. Stora negativa värden på dessa töjningar anses öka risken för initiering av en spricka. Resultaten tyder på att modellen skulle kunna användas för att förutse risken för varmsprickor och optimera fogprepareringen. För att implementera modellen i praktiska industrifall krävs dock vidare arbete. I ett möjligt fortsättningsprojekt finns det intresse av att jämföra olika materialkvalitetens inverkan på sprickrisken, simulering av fullstora komponenter och optimering av postprocessningen för att underlätta vidare implementering av modellen.

2 Executive summary in English

The purpose of this pre-study was to evaluate the possibility to use FE-simulations in order to predict the risk for hot cracks in welds in high strength steel. Avoidance of hot cracks is required in order to achieve good fatigue properties in MAG-welded joints. The cause of hot cracks is not fully investigated and today's available guidelines and tools cannot fully predict the hot crack susceptibility. It is highly possible that the cracks are non-surface breaking which implies that they can be detected with volumetric NDT-methods only, such as X-ray- and ultrasonic testing. In worst case they are found in fatigue fractures of components in use.

This project was based on physical experiments from an earlier project at Swerea KIMAB, where the impact of different base- and filler materials, as well as the impact of gap width in T-joints was evaluated with respect to hot-crack susceptibility. The main part of the simulations was based on the specimens produced in the earlier project.

The aim in this pre-study was to develop a methodology and predictive model to use as initial guidelines for minimizing the risk for hot cracks in MAG-welded T-joints. The model was verified against both specimens produced in the earlier project and against problematic applications from the industry.

It is shown in the results that it is possible to use FE-simulations in order to compare the hot crack-susceptibility in different joints. A correlation between the strains during solidification of the weld and the risk for hot cracks has been shown. The investigated strains are the ones found in the most exposed area and are directed transversal to the crack direction. It is thought that large values of these strains increase the risk for opening of a crack. The results indicate that the model can be used in order to predict the risk for hot cracks and to optimize the weld preparation. However, in order to implement the FE-simulations as a tool in the industry further investigations need to be performed. Interesting work in a continuation project can be comparison between different strength levels in both base- and filler materials, simulation of real full sized components and optimization of post processing for easier implementation.

3 Introduction

In order to reach good fatigue properties in MAG-welded joints good penetration, smooth geometries and absence of defects in the weld are required. The use of cored wires has proven to increase both the penetration and the surface smoothness compared to solid wires. However, the use of cored wires increases the risk for hot-crack formation. The reason for the increased hot-crack susceptibility for cored wires is not fully investigated and the available guidelines and tools cannot completely predict the risk. The fact that the cracks can be non-surface breaking requires the use of volumetric NDT methods, such as X-ray and ultrasonic testing, in order to investigate the quality of the weld. In worst cases the cracks are found in fatigue fractures of components in use.

This project is based on the results from a previous project at Swerea KIMAB. The previous project has investigated the hot crack susceptibility with respect to different base- and filler materials and gap widths in welded high strength steel T-joints, the set-up for the previous project is further described in chapter 4.1. This pre-study has aimed to investigate the possibility to predict the hot crack susceptibility for similar joint configurations through FE-simulations. The main goal for the project has been to develop a methodology and verify this against problematic applications from the industry and also to develop initial guidelines for minimization of the risk for hot cracks. The impact of segregation in the welded material has also been investigated.

4 Background

4.1 Physical experiments from earlier study

This chapter describes briefly the experiments performed in the earlier study. These experiments have been the base for the FE-simulations performed in this project. The experiments have been performed with two different base materials and four different filler materials.

The experimental set-up is based on earlier trials performed at Volvo; a schematic illustration of the trials at Volvo can be seen in Figure 1. Seven grooves were milled out in the web plate in order to represent different gap sizes. An illustration of the web plate can be seen in Figure 2.

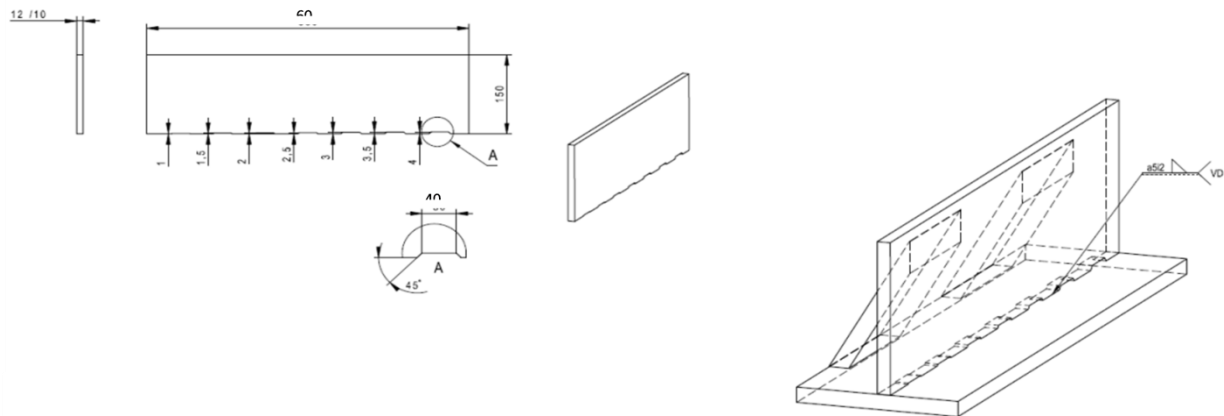


Figure 1. Schematic illustration of the experimental set-up from the trials at Volvo.

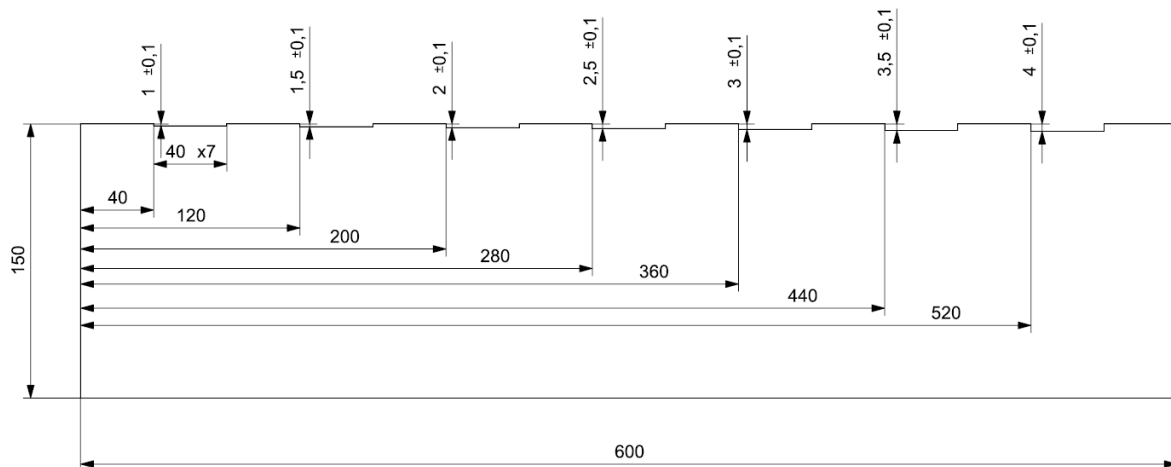


Figure 2. Illustration of milled grooves in the web plate.

As shown in Figure 1, the Volvo trials used 45° angled brackets welded to the backside of the web plate for fixation. A different set-up for the fixture was used in the experiments in this project, the fixture can be seen in Figure 3.

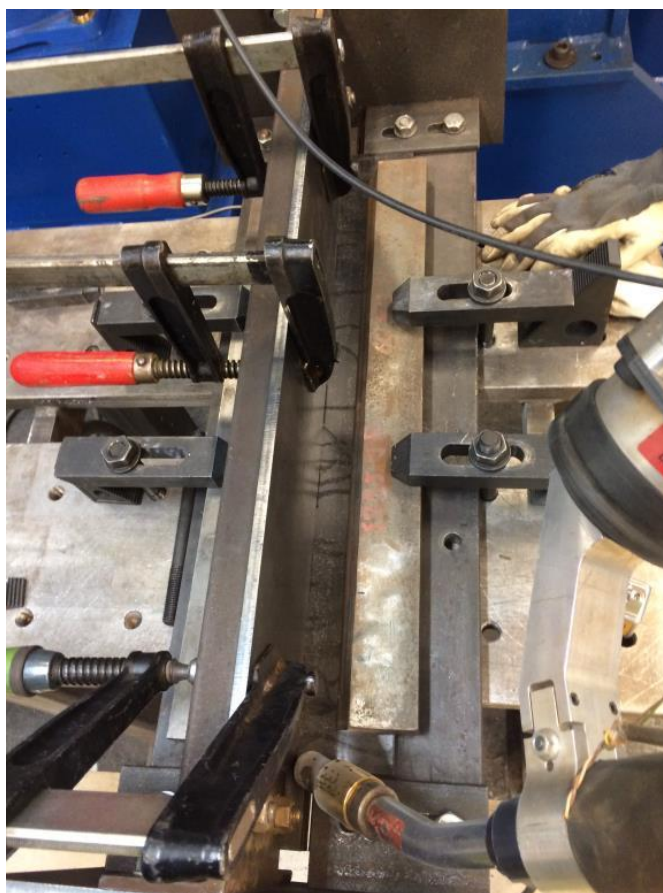


Figure 3. Fixture used in the welding trials.

The pre-study focused mainly on two of the welding series produced in the previous project. The difference between the two series was the aim of the welding torch. The two different aims are illustrated in Figure 4. The results from the previous project had shown that the hot-crack susceptibility decreased when the torch was aimed at the lower corner of the web plate, Figure 4a, compared to the lower aim at the intersection point between the web plate and the base plate, Figure 4b.

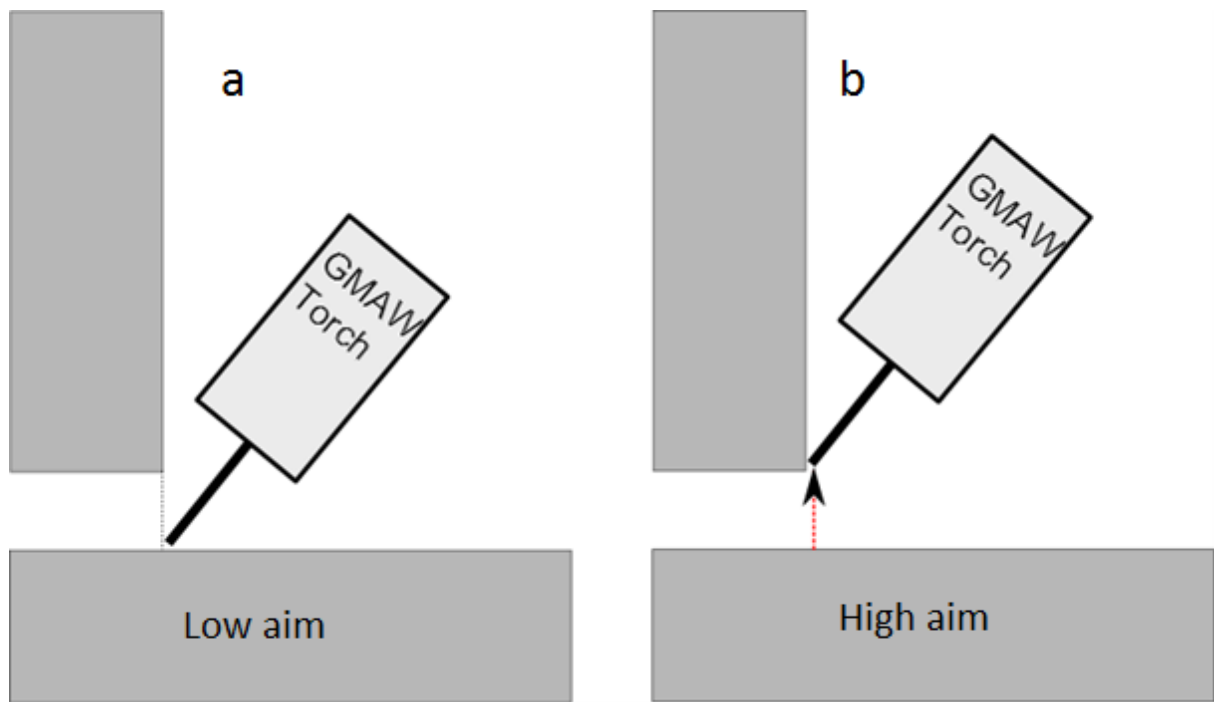


Figure 4. Illustration of the two different aims.

Images of the cross-sections from the two different series can be seen in Figure 5, the series welded with low aim, and Figure 6, the series welded with high aim.

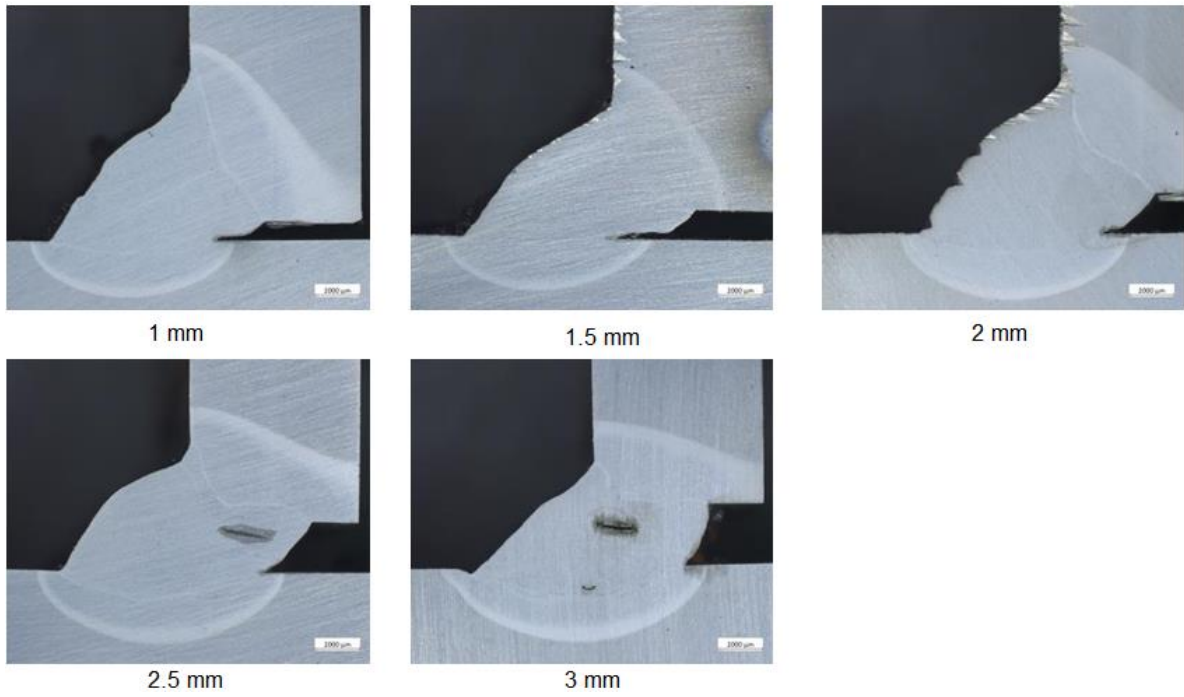


Figure 5. Cross-sections from series welded with low aim.

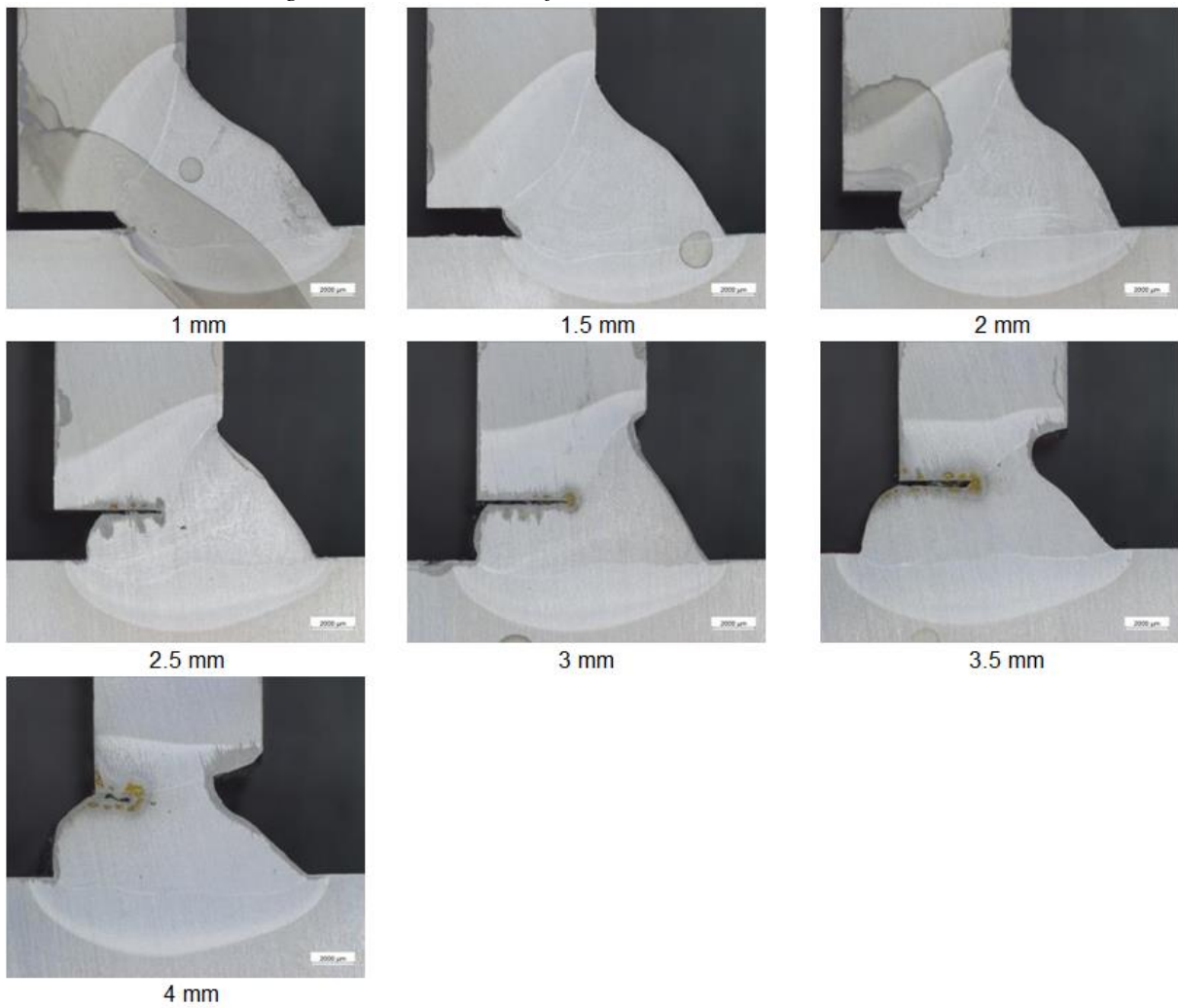


Figure 6. Cross-sections from series welded with high aim.

4.2 Materials

The base materials in this project was, STRENX 900 MC and STRENX 900 plus from SSAB. The filler materials were OK AristoRod 89 and OK Coreweld 89 from ESAB and BÖHLER kb 90 T-FD and BÖHLER 900 T-MC from Voestoalpine böhler.

The mechanical properties and chemical compositions for the steels and filler wires are shown in Table 1 and Table 2. The shielding gas, from AGA-Linde Gas, used in the tests is shown in Table 3.

Table 1: Mechanical properties of the base and filler materials.

Grade	Thickness/ diameter (mm)	Batch/lot no.:	Surface treatment	R _{p0.2} (MPa)	R _m (MPa)	A ₅ (%)	Temp °C	Energy MV (J/cm ²)	Energy MV (J)
Materials									
STRENX 900 MC	8	48370-021	As rolled	-	-	-	-	-	-
STRENX 900 plus	8	724577	As rolled	-	-	-	-	-	-
Filler metal									
OK Coreweld 89	1.2	PV1080191							
OK AristoRod 89	1.2	PV608071270B		700*	900*		-30*		60*
BÖHLER kb 90 T-FD	1.2	552212		≥890	940-1180		-40*		≥47
BÖHLER 900 T-MC	1.2	639812		≥890	940-1180	≥15	-60*		≥47

*Nominal values

Table 2: Chemical analysis of the base material and the filler material.

Analysis (wt-%)	Fe	C	Si	Mn	P	S	N	Al	Cr	Ni	Cu	Mo	Nb	V	Ti	B	Sn	CE	CET
STRENX 900 MC	Bal	0.09	0.04	1.08	0.009	0.001	0.004	0.04	1.11	0.058	0.015	0.12	0.002	0.01	0.015	0.0017	0.002	-	-
STRENX 900 plus	Bal.	0.16	0.3	1.3	0.01	0.001	0.003	0.032	0.16	0.06	0.01	0.4	0.001	0.01	0.01	0.0016	0.002	0.5	-
OK Coreweld 89	Bal.	0.081	0.53	1.217	0.01	0.015	-	-	0.49	2.738		0.734	0.01	0.01	-	-	-	-	-
OK AristoRod 89	Bal.	0.113	0.81	1.9	0.01	0.005	0.004	0.008	0.37	2.16	0.137	0.561	0.008	0.007	0.055	-	0.004	-	-
BÖHLER kb 90 T-FD	Bal.	0.08	0.27	1.42	0.011	0.008	-	-	1.01	2.15	<0.1	0.4	-	<0.01	-	-	-	-	-
BÖHLER 900 T-MC	Bal.	0.08	0.48	1.62	0.012	0.009	-	-	0.38	2.51	<0.1	0.51	-	<0.01	-	-	-	-	-

Table 3: Shielding gases and composition of gases used in the project.

Product	Composition (vol-%)			
	Ar	CO ₂	He	NO
AGA MISON 18	Bal.	18	-	0.03

5 Method

5.1 Thermodynamic calculations

Solidification cracking in welds occur during the final stages of solidification when tensile shrinkage stresses accumulate in the liquid film still present along the solidification grain boundaries [1][2][3]. The cracks are located in the fusion zone. The temperature range associated with solidification cracking is referred to as the Brittle Temperature Range (BTR) [1][4]. The value can be defined as the difference between liquidus and solidus temperature and is also called solidification temperature range. The solidus temperature is usually defined by the lowest melting eutectic in the system. A classic example of this is the effect of Sulphur (S) and Phosphorus (P) on the cracking susceptibility of Fe- and Ni based alloys. S can reduce the solidus temperature significantly. The width of the BTR can be used as a measurement of cracking susceptibility [4][2]. Generally speaking, the wider the BTR, the larger the area that is weak and susceptible to weld-solidification cracking [5].

Several factors could affect solidification cracking susceptibility. Solidification temperature range, amount and distribution of liquid at the terminal stage of solidification, the primary solidification phase, grain structure, ductility of the solidifying liquid, thermal expansion, degree of restraint. A general conclusion is however that a minimized solidification range helps to decrease solidification cracking susceptibility [3].

In this project the commercial software ThermoCalc was used to calculate the solidification range and indicate segregation of different alloying elements in the investigated base and filler materials. To estimate the

solidification range the so called Scheil-Gulliver method was used. The Scheil-Gulliver method allows calculation of the fraction and composition of all phases during solidification step by step from the liquidus temperature to the temperature where solidification of the residual liquid phase occurs.

The calculated solidification ranges was not used as a measure directly correlated to hot cracking susceptibility but merely as an aid to draw conclusions together with other results.

5.2 Analysis of welded material and crack surfaces

In order to examine the occurring cracks in the specimens a number of different analysis methods were used. The crack surfaces from the specimens in the earlier project were broken open with a hydraulic press and examined by Scanning Electron Microscopy analysis (SEM) in order to investigate whether the cracks did originate from the solidification of the weld or if it was another type of cracks. The specimens were also analysed with Energy Dispersive X-ray Spectrometry (EDS), which calculates the amount of each element in each analysed point. This analysis was performed in order to investigate if a noticeable segregation of elements had occurred, which in turn could be the reason for hot cracking. The elements in focus for the analysis were Sulphur (S), since these elements are reported to have large influence on the cracking susceptibility.

5.3 FE-simulations

All the welding simulations were performed with the commercial FE-software Sysweld. The aim with the simulations was to calculate the thermal and mechanical history for the welds, and investigate if the stress- and strain levels could be correlated to the presence of hot cracks from the physical experiments. The thermal and mechanical properties of the materials were obtained from the Sysweld database.

The first part of the simulations was performed with 2D-models in order to decrease the computation time. The set-up of the 2D-model was performed by setting the initial temperature of the welded material to 1500°C and the initial temperature of the base material to 20°C. However, this model was found to be too simplified and no correlation regarding hot crack susceptibility could be seen between the simulations and the physical tests.

In order to better simulate the heat source, the thermal conduction in the material and the mechanical mechanisms a 3D-model was set up. The heat source was represented by a double-ellipsoid in the simulations. The geometry and position of the double-ellipsoid was adjusted in order to achieve a weld penetration profile similar to the cross-sections from the physical experiments. The results from the simulation are further described in chapter 6.3.

6 Results

6.1 Thermodynamic calculations

The ratio of Manganese and Sulphur in the weldment is often considered one important factor for hot cracking susceptibility. One recommendation to avoid hot cracking issues is to keep the Mn/S ratio > 20. The role of Sulphur on the solidification range is shown in the equilibrium calculations of the solidus and liquidus temperature as a function of Sulphur content in a fictive C-Mn steel in Figure 7. At low Sulphur concentrations, the Sulphur is bound to Manganese in the form of MnS particles and does not affect the solidification range in a significant way. As the Sulphur content increase there is not sufficient amount of Manganese to keep forming MnS particles, thus resulting in an excess of Sulphur. Instead the Sulphur reacts with Fe forming low melting phases such as FeS which greatly increases the solidification range of the alloy. The figure clearly shows the effect of increased Sulphur content on the solidification range and the importance of keeping track of the Mn/S ratio. The calculations shown in Figure 7 are equilibrium calculations and both Sulphur and Manganese are elements that are expected to segregate during solidification. It is thus important to note that very high Sulphur contents can be found in the last solidifying fraction of the melt although the average Sulphur concentration in the alloy is relatively low.

2017.02.24.21.32.43

TCFE7: C, CR, FE, MN, MO, NI, S, SI

N=1., P=1E5, W(C)=8.1E-4, W(SI)=8E-3, W(NI)=2.22E-2, W(MO)=5.33E-3, W(MN)=1.75E-2, W(CR)=4.1E-3

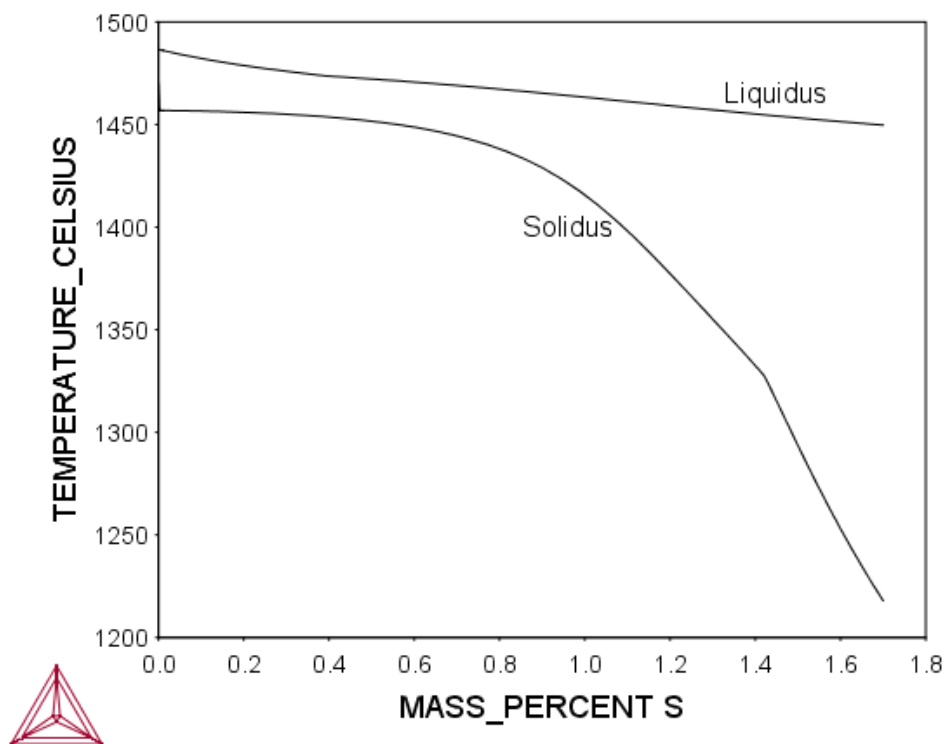


Figure 7: Equilibrium calculation of liquidus and solidus lines for a fictive C-Mn steel composition as a function of Sulphur content in the steel.

In Figure 8 the segregation of alloying elements in a typical filler material used in this study is shown. Mn, S, C, Mo, Si are all elements that are expected to segregate to the last solidifying melt, whereas Ni and Cr show less tendency for segregation.

2017.02.23.22.25.30
 TCFE7: C, CR, FE, MN, MO, NI, SI
 T=1783.42, W(C)=7E-4, W(SI)=4E-3, W(NI)=2.2E-2, W(CR)=5E-3, W(MO)=4E-3, W(MN)=1.4E-2, P=1E5, N=1

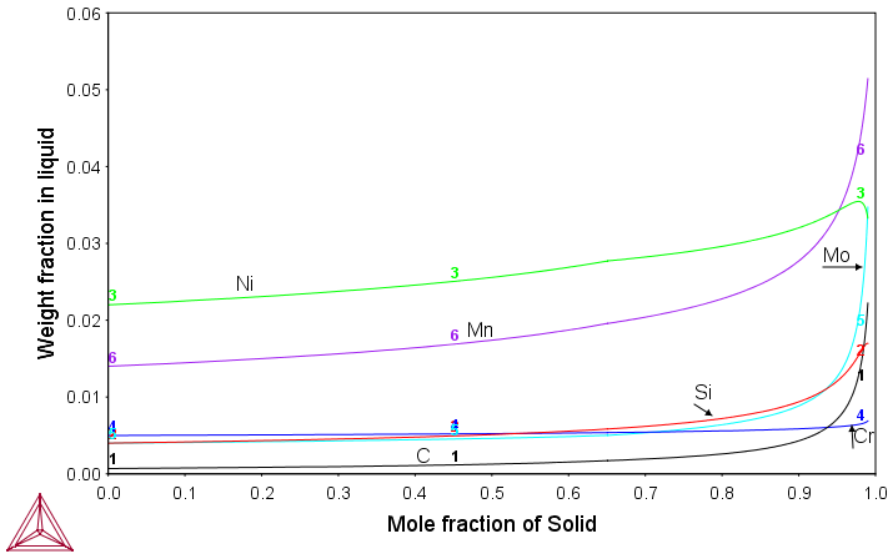


Figure 8 Segregation of alloying elements in a typical filler material used in this study

The results obtained in Figure 8 can also be plotted as solidification temperature vs. mole fraction solid as seen in Figure 9. This gives an indication of how the element segregation affects the solidus temperature for this specific alloy at different fractions of solidified melt. From this information the solidification range is calculated by subtracting the temperature at 95% solid fraction from the liquidus temperature (temperature at zero fraction solid).

2017.02.23.22.31.28
 TCFE7: C, CR, FE, MN, MO, NI, SI
 T=1783.42, W(C)=7E-4, W(SI)=4E-3, W(NI)=2.2E-2, W(CR)=5E-3, W(MO)=4E-3, W(MN)=1.4E-2, P=1E5, N=1

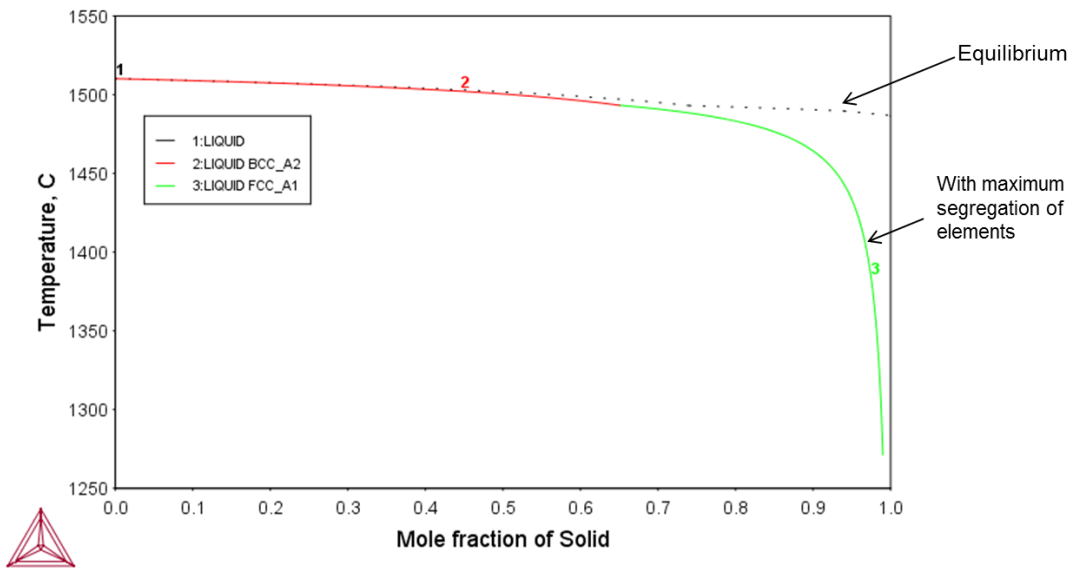


Figure 9 Solidification range of the same alloy used for calculations in Figure 8

Figure 10 shows the solidification range for all alloys (base and fillers) used as input to this study. These solidification ranges has not been directly used to determine the risk for solidification cracking but has instead been used in combination with other results to make reasonable explanations for the experimental results.

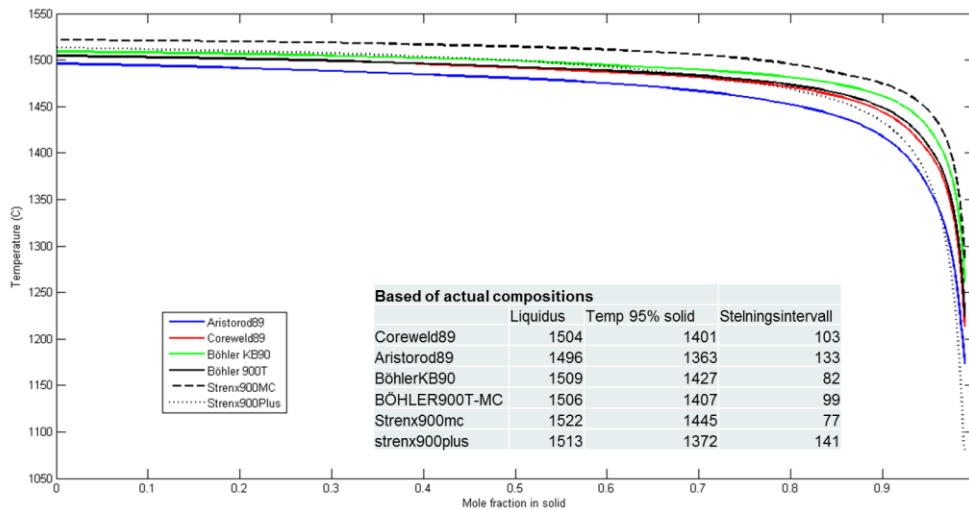


Figure 10 Solidification range for all base and filler materials used in this study

6.2 Analysis of welded material and crack surfaces

Figure 11 shows the crack surface of an opened specimen, the crack surface is marked red in the figure.



Figure 11, A hot crack that has been broken open, the crack is marked with the red line

The SEM-analysis from the specimen can be seen in Figure 12. The figure does also show the cross-section from the analysed specimen. The results from the SEM-analysis concluded that the cracks originated from the solidification and hereby were proven to be hot cracks.

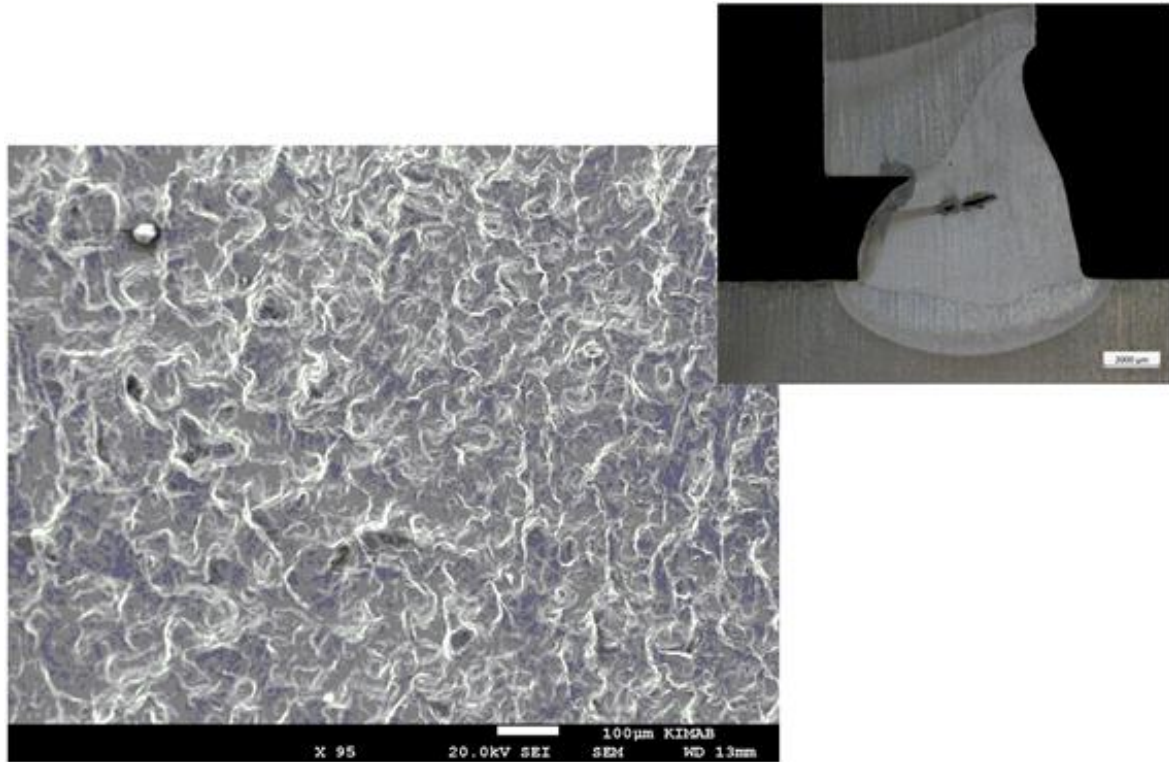


Figure 12, SEM analyzed surface of the crack in weld 63.

The results from the EDS-analysis of the crack surface can be seen in Figure 13. One issue with the EDS-method is the fact that the emitted energies from Sulphur and Molybdenum overlaps, which in turn complicates the analysis of the results.

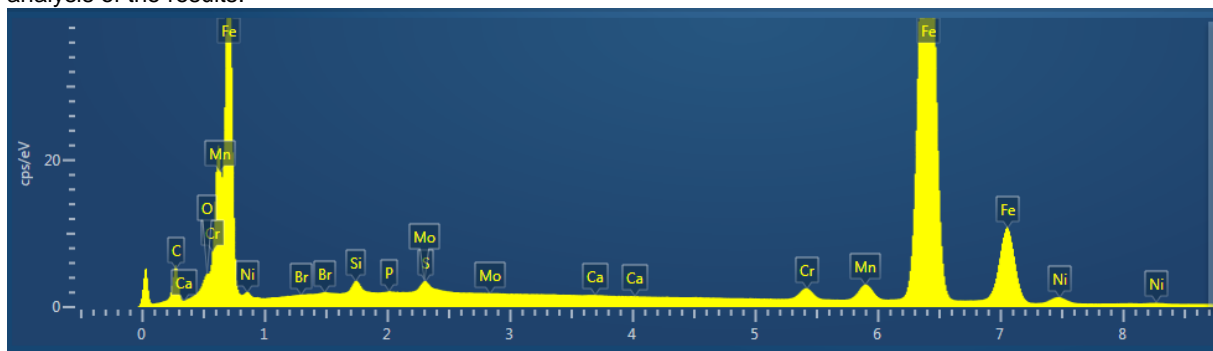


Figure 13, EDS analysis of the elements on the crack surface.

In order to better analyse the segregation phenomenon Wavelength Dispersive X-ray Spectroscopy (WDS) was used. The mapping was performed on cross-sections of two welded specimens, one with a centreline crack and one without any crack. The results from the analysis can be seen in Figure 14. The results do not show any clear indications of segregation, which in turn demonstrates that the hot crack susceptibility cannot only be explained by segregation.

WDS (S, Mo) + EDS point analysis along a line

20 kV, 64 nA, WD=14 mm, A-B line length 12 mm, 240 analysis points, every 50 μm

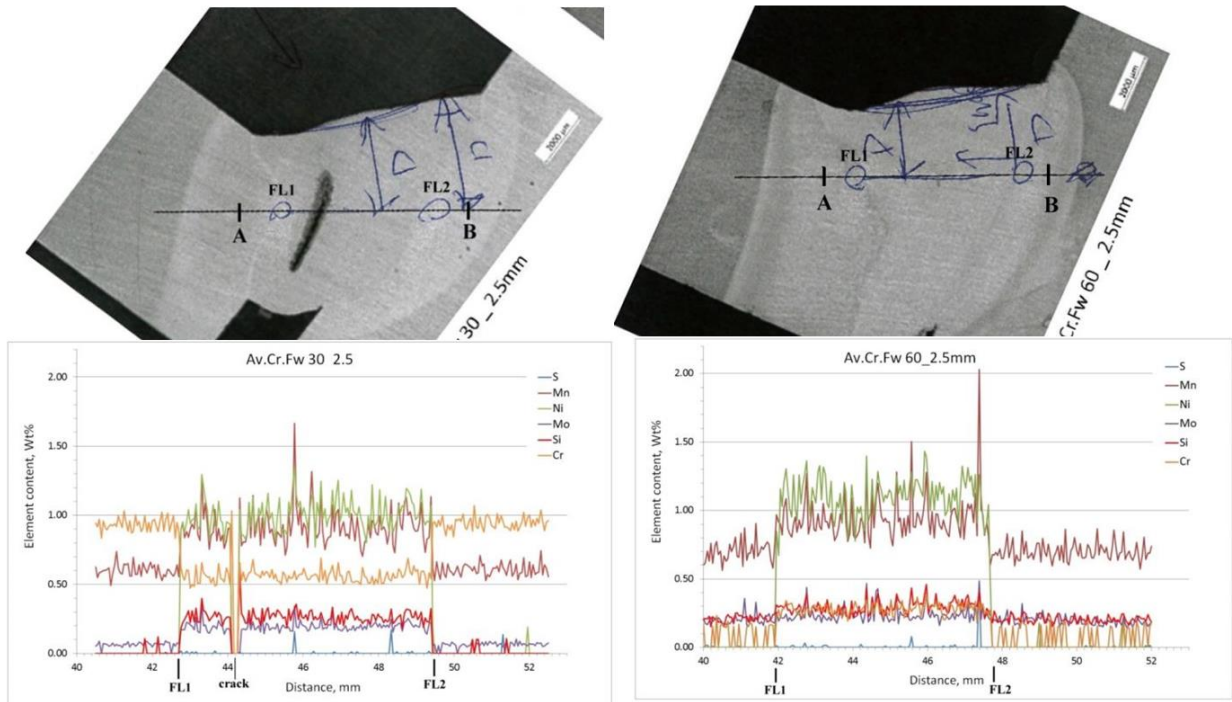


Figure 14, WDS analysis along a line across the cross sections.

6.3 FE-simulations

The FE-simulations were performed in order to evaluate if the cracks could be explained by mechanical impact of the material during solidification. The simulations were performed both with 2D- and 3D-models.

6.3.1 2D-simulation

The 2D-simulations were based on the cross-section shown in Figure 15. This specimen was welded with low aim and a 1 mm gap between the web plate and the base plate. The 2D-model mesh can be seen in Figure 16.

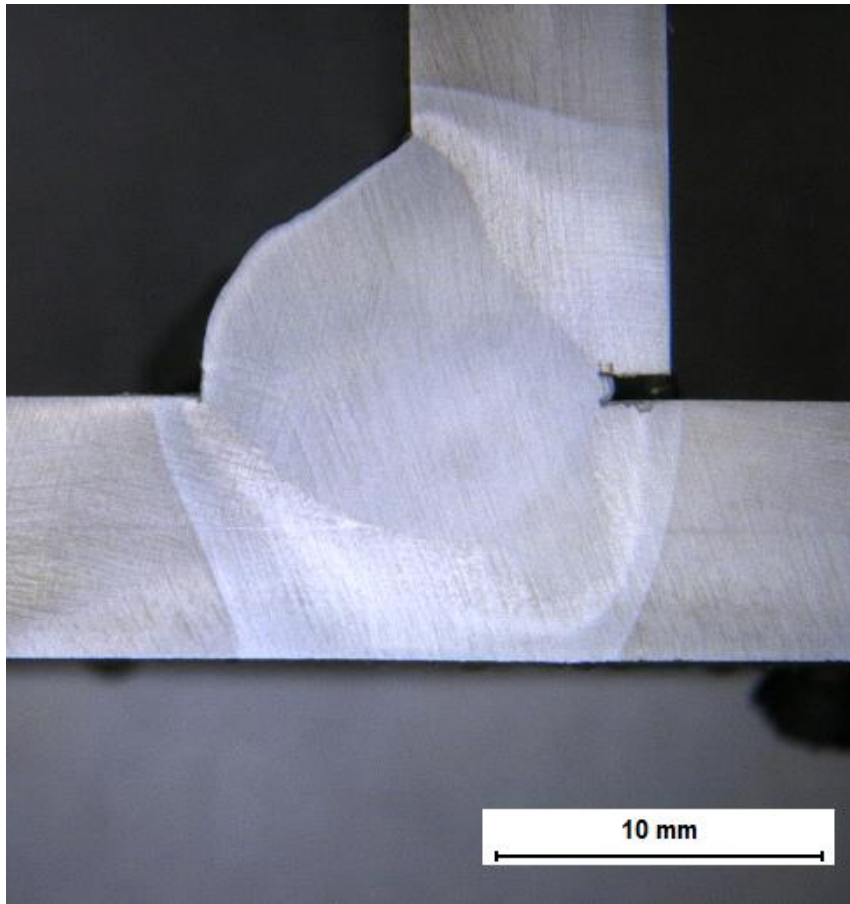


Figure 15. Cross-section of weld used for 2D-simulations.

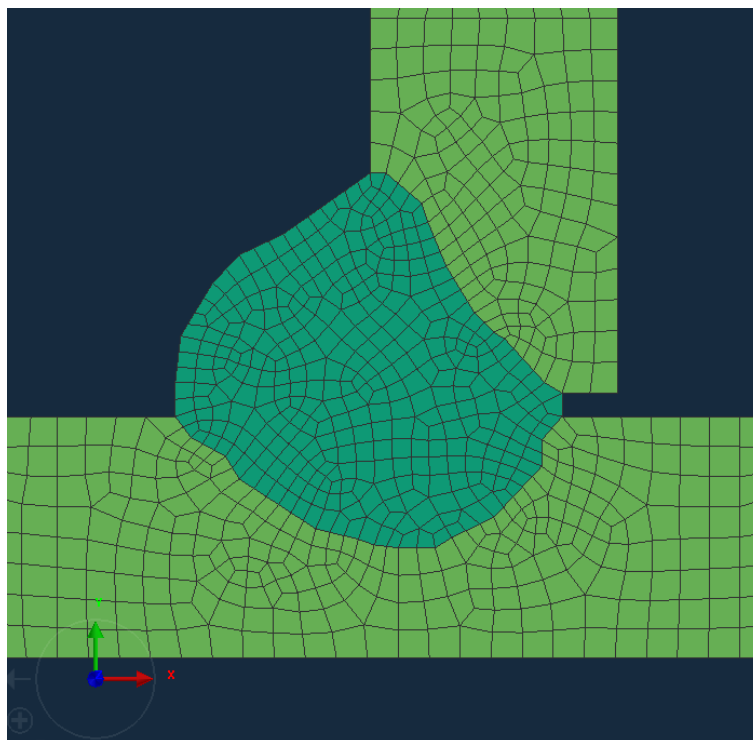


Figure 16. 2D-model mesh.

The strain distribution from the 2D-simulation can be seen in Figure 17. The strain is measured perpendicular to the direction which is thought to be most prone to form a hot crack, illustrated by the red line in the image.

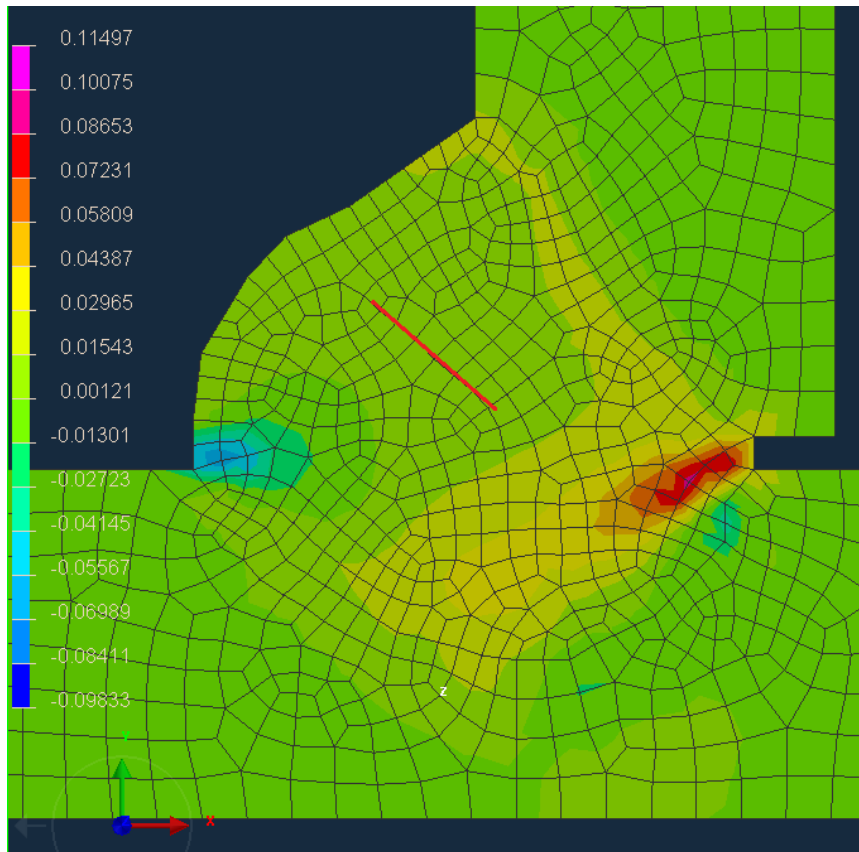


Figure 17. Strain distribution from 2D-simulations.

The maximum negative strain is the entity which is thought to be of main interest, since it is the shrinkage in the material which is thought to cause the hot cracks. Since the results from the 2D-model did not show any capability to predict the risk for hot cracks the rest of the project focused on 3D-modeling. The insufficient accuracy of the 2D-model is thought to derive from both the fact that no heat source is applied in the model, which in turn leads to an instantaneous heating of the material, and that no heat conduction takes place in the direction of the weld.

6.3.2 3D-simulations – cases from previous project

The 3D-simulations were based on cross-sections from the physical trials. The cross-sections shown in Figure 18 were used for the first part of the 3D-simulations. These specimens consist of the same base- and filler material and are produced with the same gap, 2,5 mm. The cross-section shown in Figure 18a was welded with low aim of the torch and the cross-section shown in Figure 18b was welded with high aim of the torch.

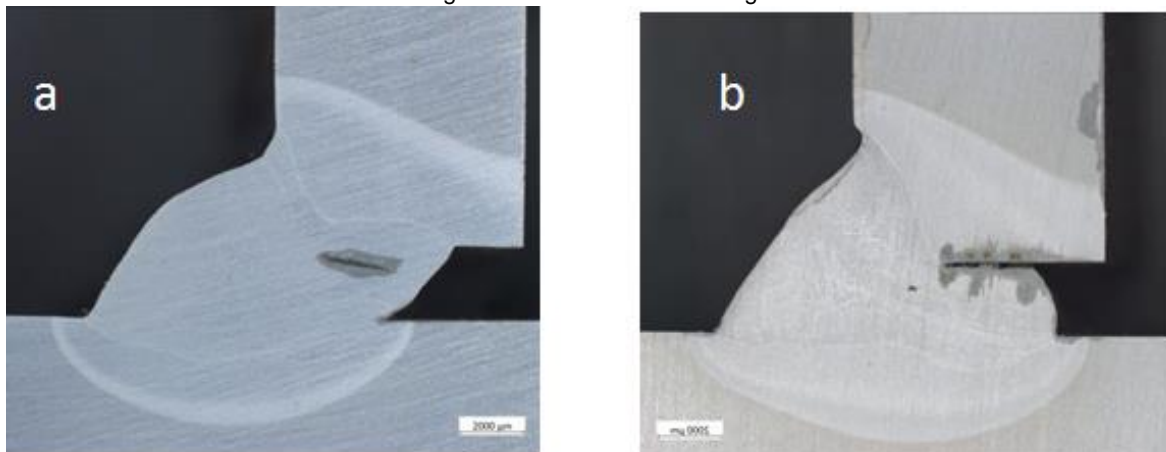


Figure 18. Cross-sections of welds for 3D-simulations. The welds are produced with the same base- and filler material. Specimen (a) is welded with low aim of the torch and specimen (b) is welded with high aim of the torch.

The meshes for the two specimens are shown in Figure 19 and Figure 20. The red lines illustrate the areas which are found to be exposed to the largest strains.

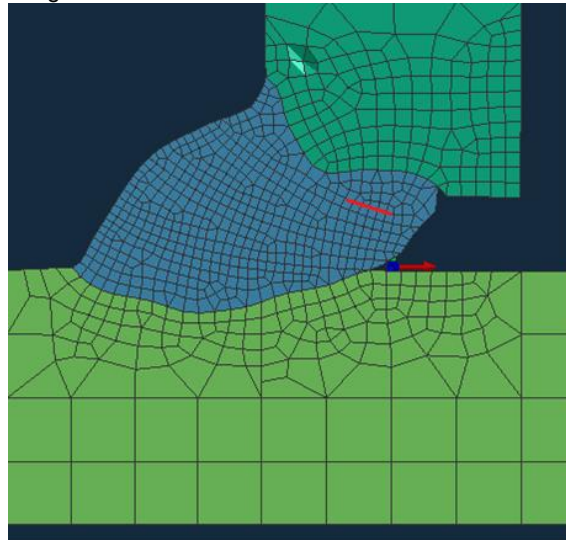


Figure 19. Image showing the mesh of the specimen from the first part of the 3D-simulations, specimen welded with low aim of the torch.



Figure 20. Image showing the mesh of the specimen from the first part of the 3D-simulations, specimen welded with high aim of the torch.

Illustrations of the strain distributions in the two cases can be seen in Figure 21 and Figure 22. The continuous strain distribution in the areas of interest is shown in Figure 23 and Figure 24.

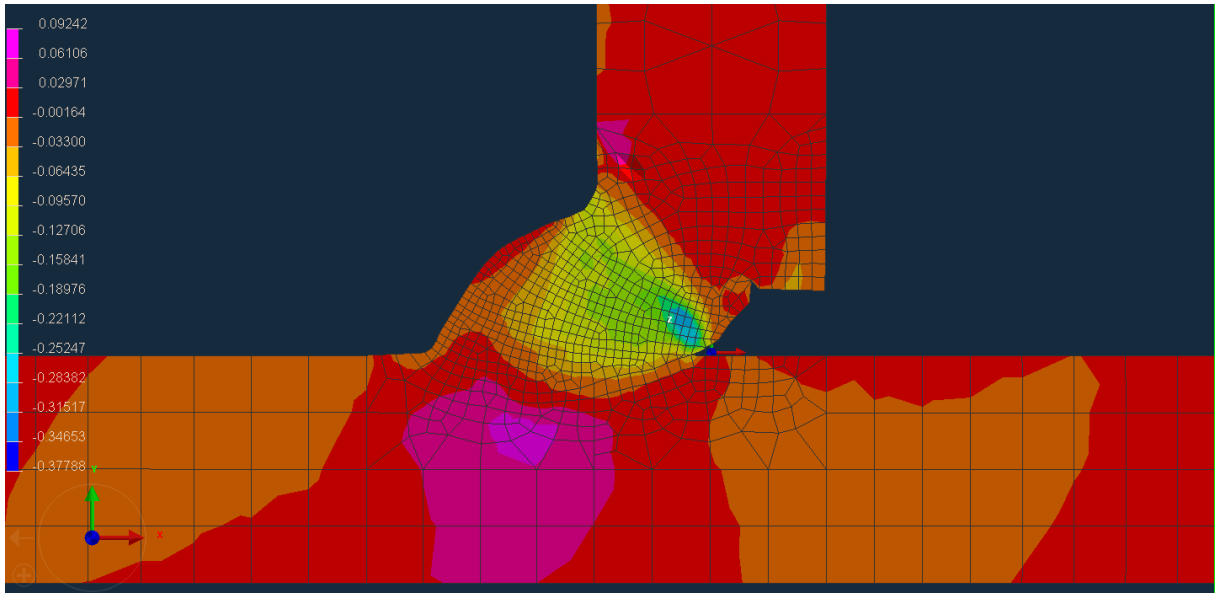


Figure 21. Strain distribution for case with low aim.

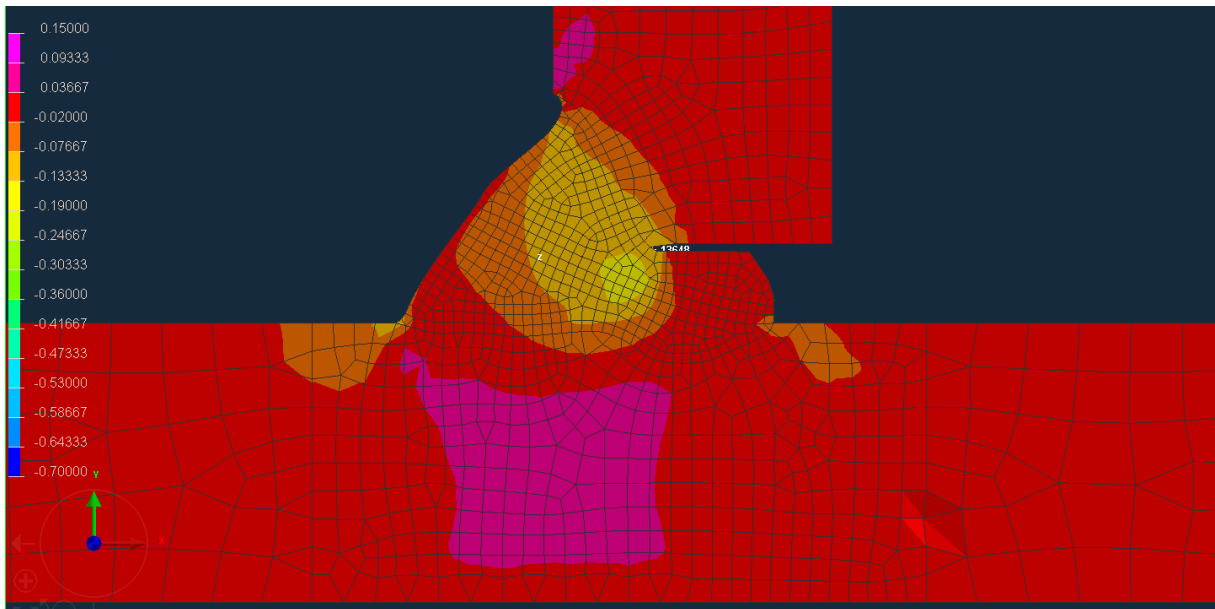


Figure 22. Strain distribution for case with high aim.

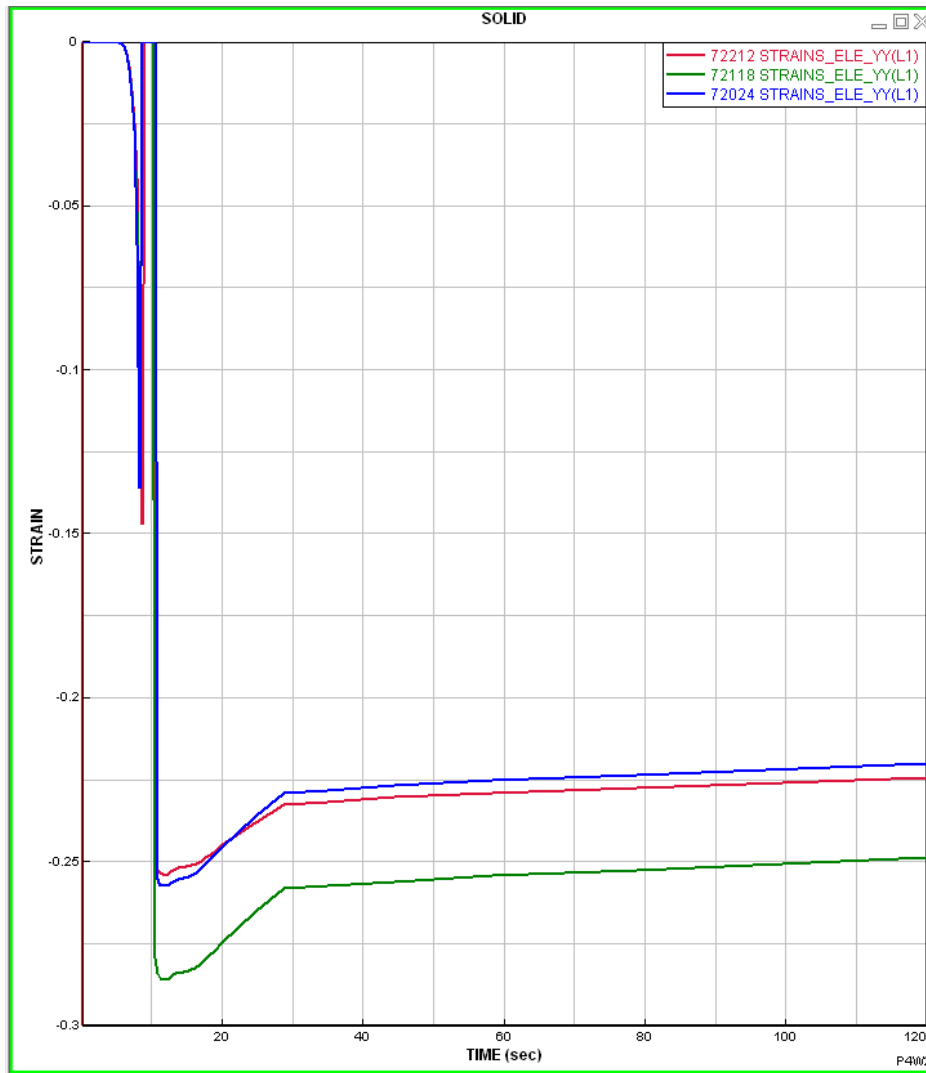


Figure 23. Continuous strain for elements in area most prone to form hot cracks for specimen welded with low aim.

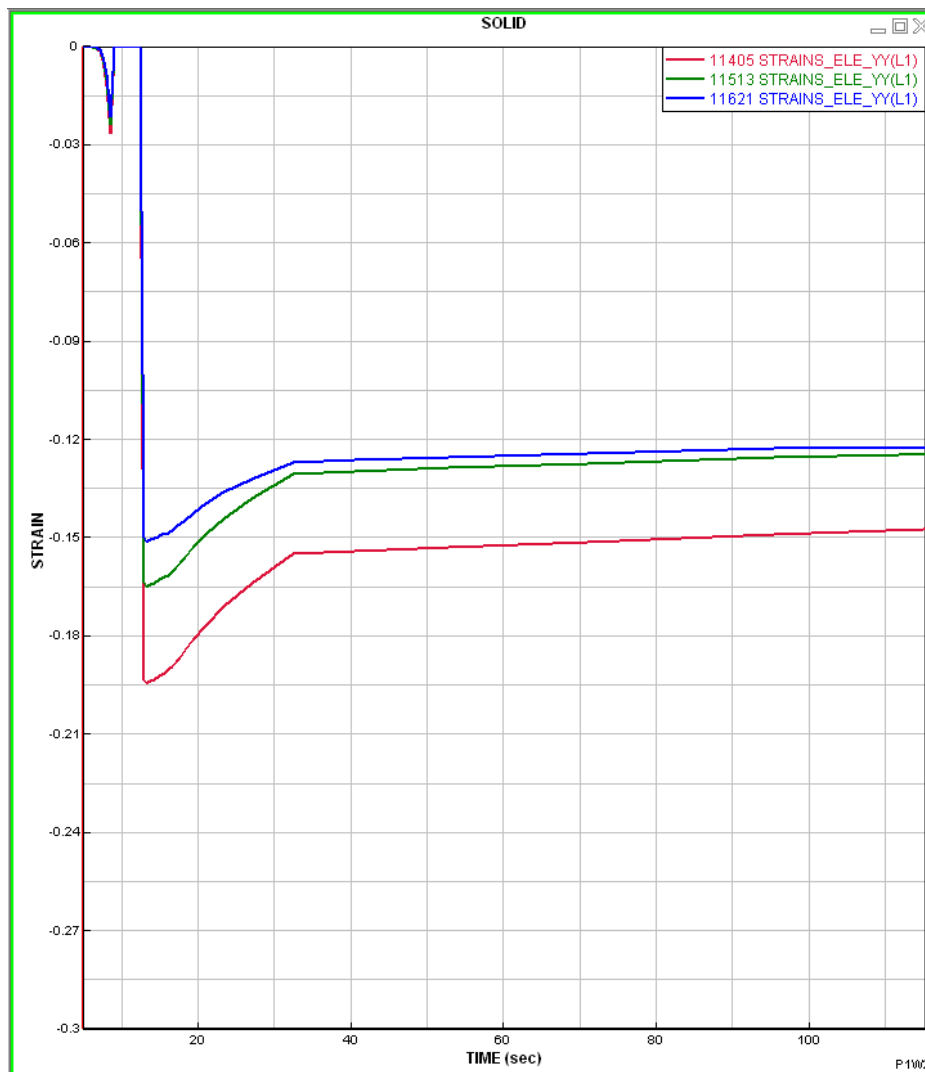


Figure 24. Continuous strain for elements in area most prone to form hot cracks for specimen welded with high aim.

While comparing the graphs in Figure 23 and Figure 24 it can be seen that the specimen welded with low aim is exposed to a larger strain compared to the specimen welded with high aim. It can also be seen in Figure 21 that the maximum negative strains occurs in the area close to the crack shown in Figure 18a.

6.3.3 3D-simulations – industrial cases

The specimens shown in Figure 26-Figure 29 were provided by Huddig. The first two specimens were prepared with half V-joints, 0 and 2,5mm gap respectively. The second two specimens were prepared with half V-joints with land, illustrated in Figure 25, also prepared with gaps of 0 and 2,5mm respectively.

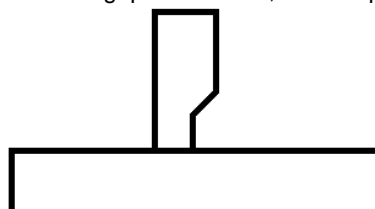


Figure 25. Illustration of joint preparation for half V-joint with land.

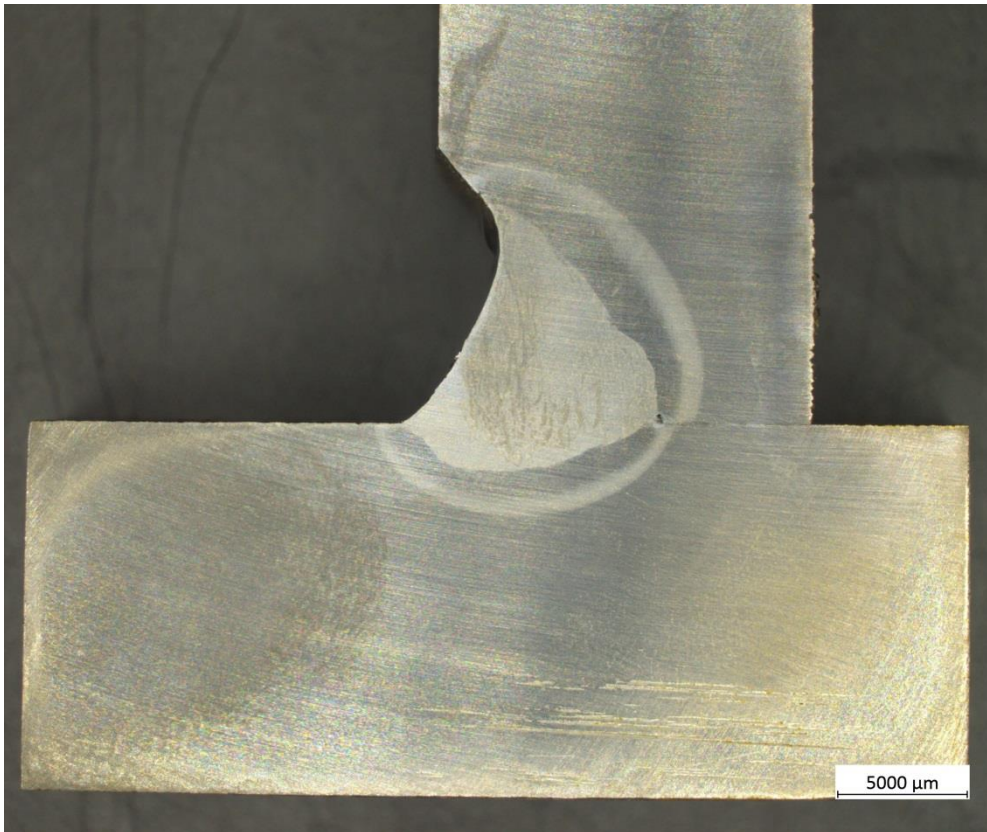


Figure 26. Specimen welded at Huddig, half V-joint and 0mm gap.

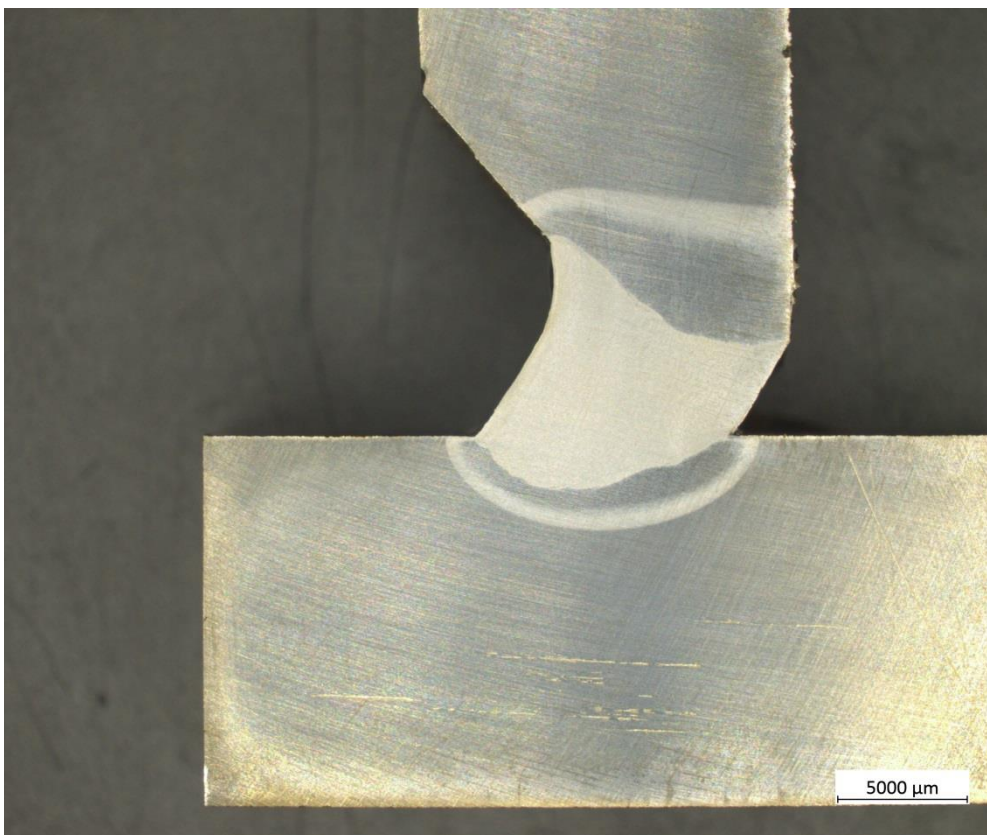


Figure 27. Specimen welded at Huddig, half V-joint and 2,5mm gap.



Figure 28. Specimen welded at Huddig, half V-joint with land and 0mm gap.

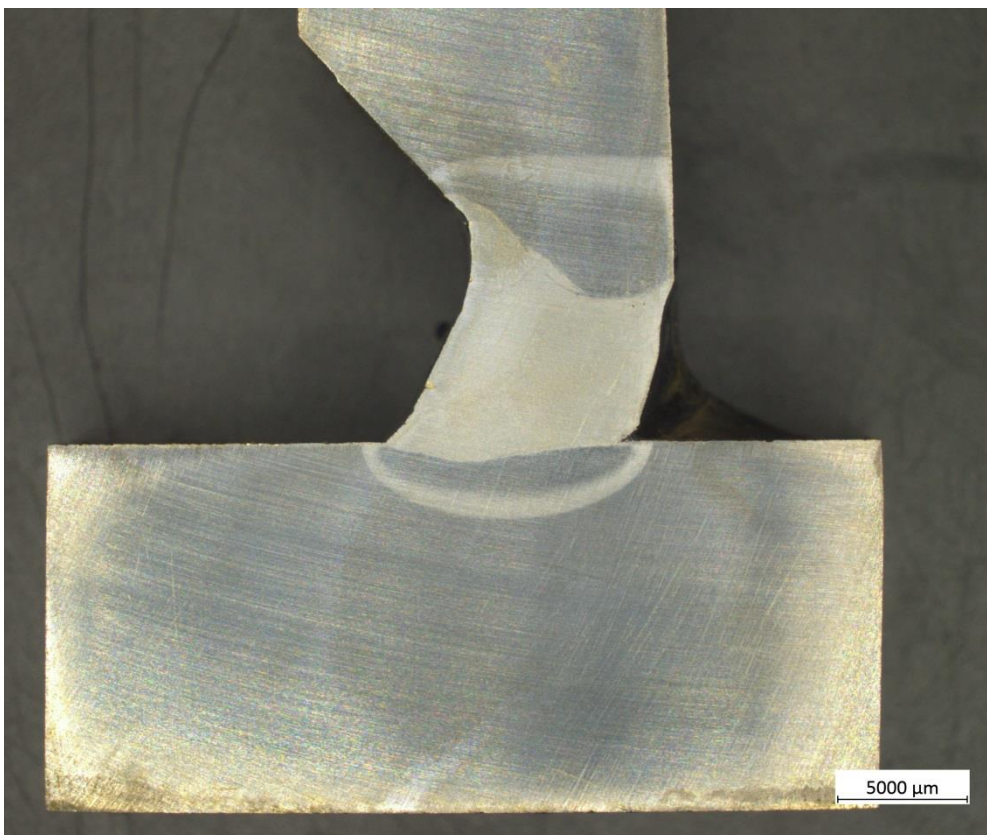


Figure 29. Specimen welded at Huddig, half V-joint with land and 2,5mm gap.

The strain distribution for the two cases prepared with half V-joint can be seen in Figure 30 and Figure 31. The red circles display the areas which are found to be of most interest. The continuous strains in these elements are shown in Figure 32 and Figure 33.

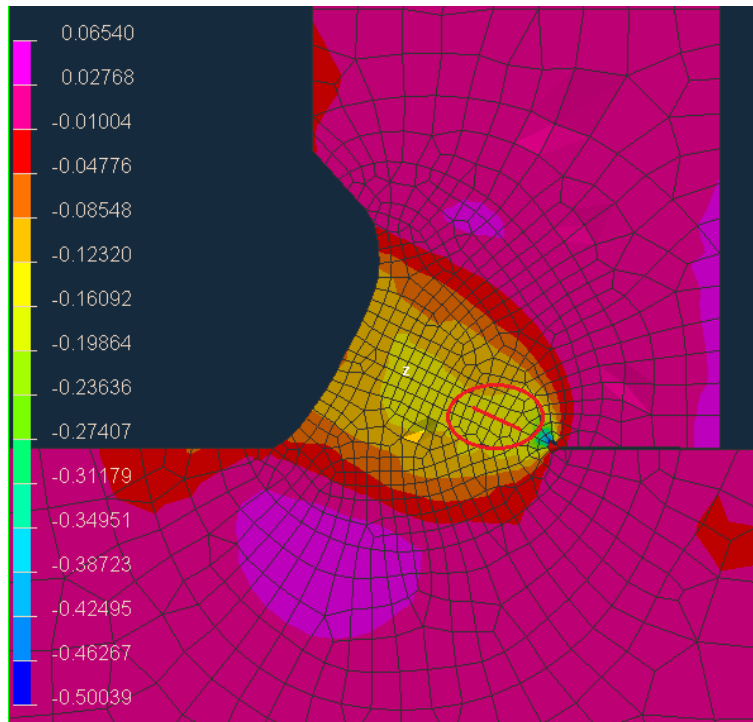


Figure 30. Strain distribution in specimen welded with half V-joint and 0mm gap. Area of interest marked in red circle.

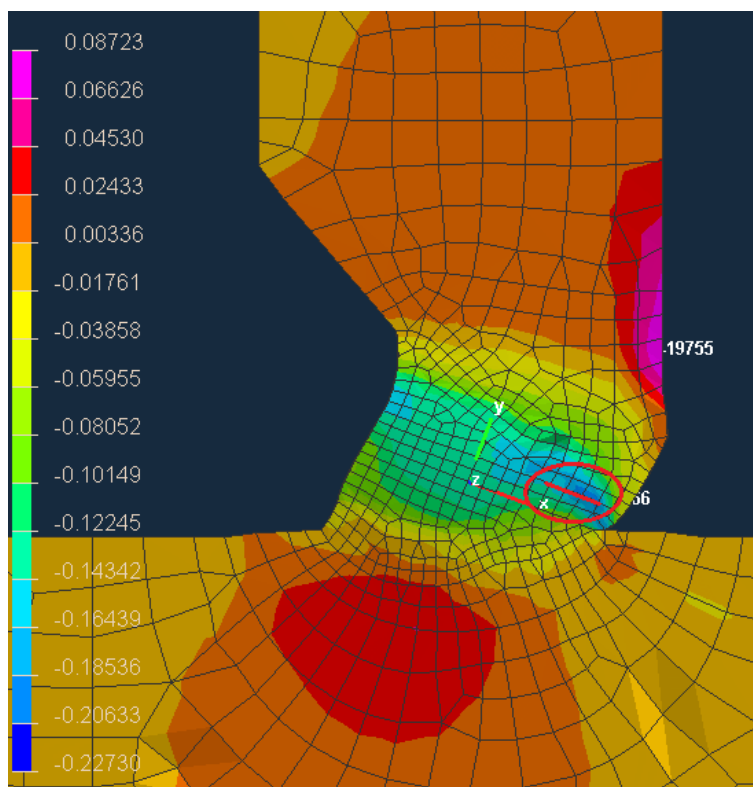


Figure 31. Strain distribution in specimen welded with half V-joint and 2,5mm gap. Area of interest marked in red circle.

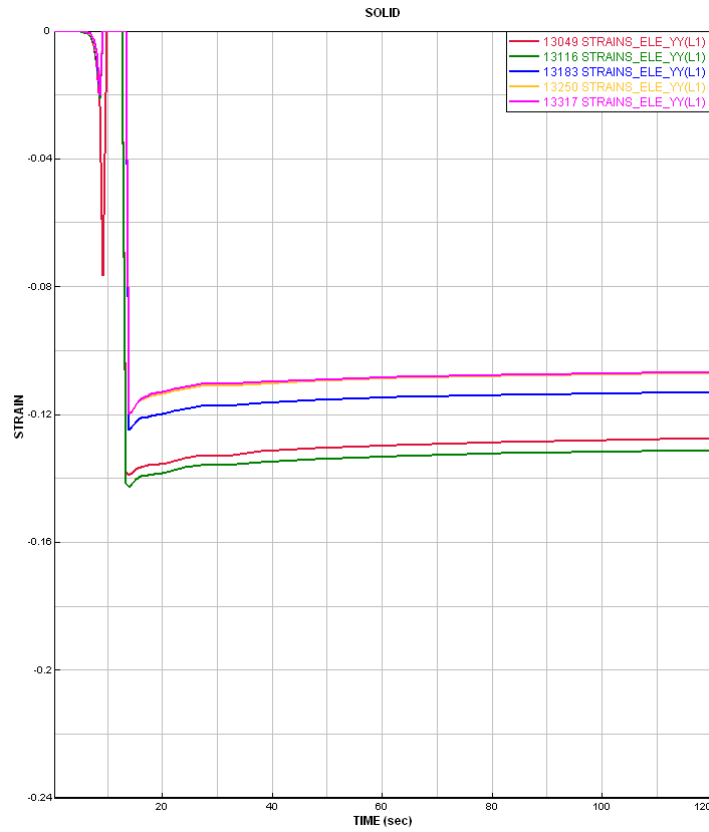


Figure 32. Continuous strain in elements marked with red in Figure 30.

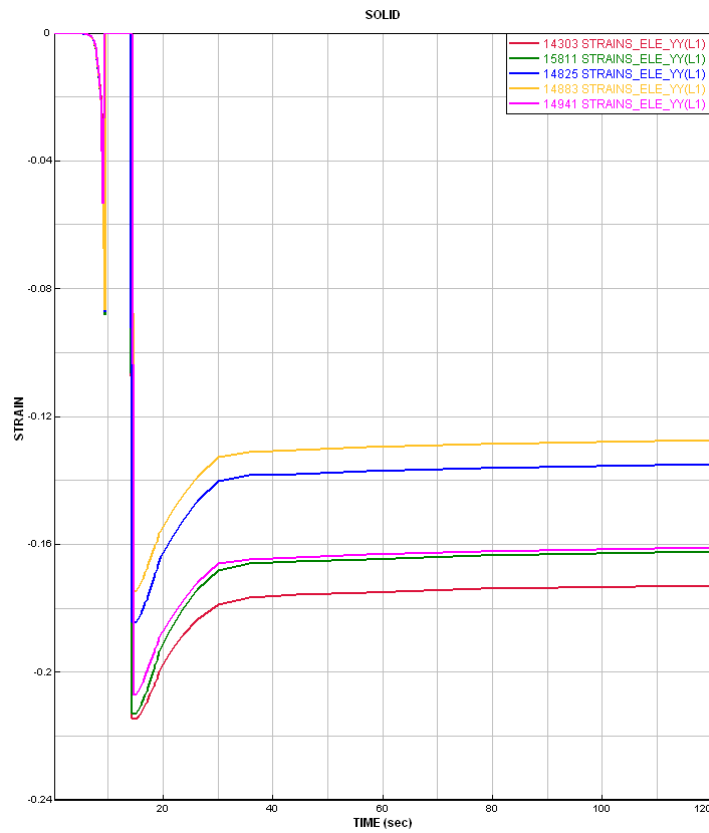


Figure 33. Continuous strain in elements marked with red in Figure 31.

The strain distribution in the two cases prepared with half V-joint with land can be seen in Figure 34 and Figure 35. The red circles shows the areas which are found to be most exposed for cracking. The continuous strains in these elements are shown in Figure 36 and Figure 37.

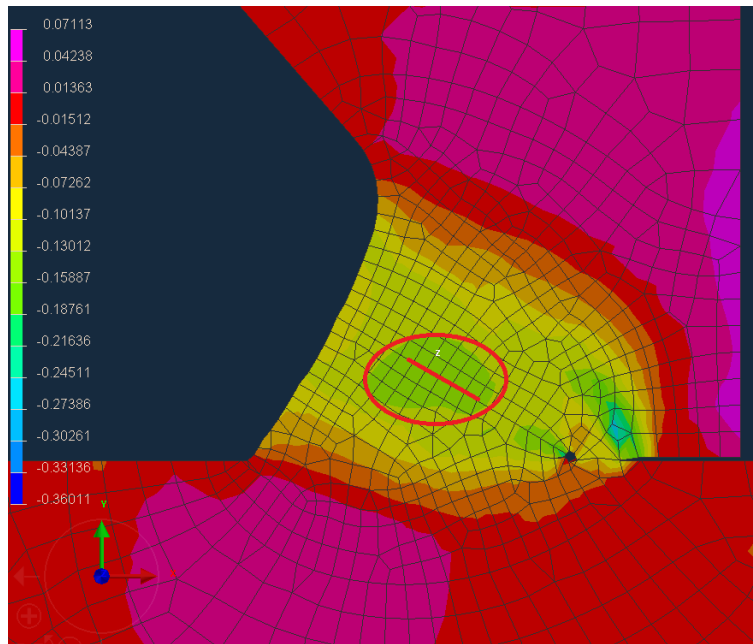


Figure 34. Strain distribution in specimen welded with half V-joint with land and 0mm gap. Area of interest marked in red circle.

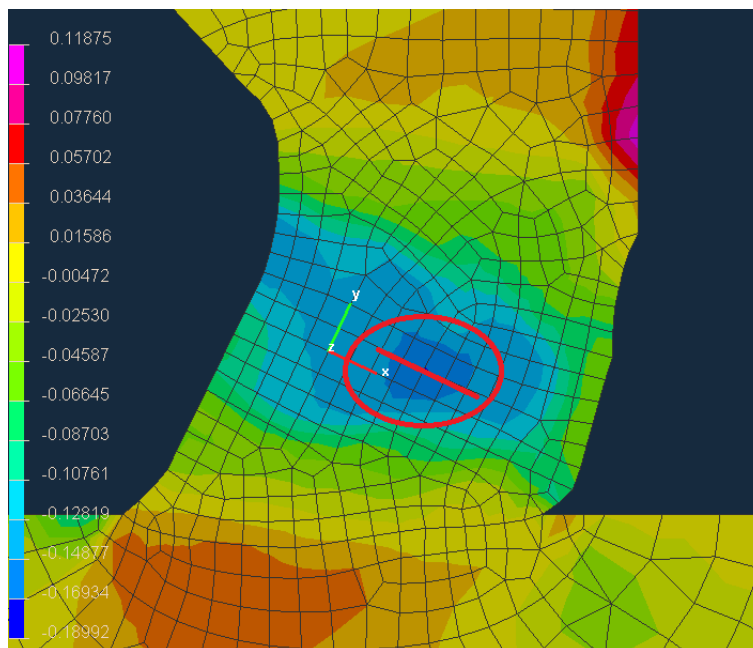


Figure 35. Strain distribution in specimen welded with half V-joint with land and 2,5mm gap. Area of interest marked in red circle.

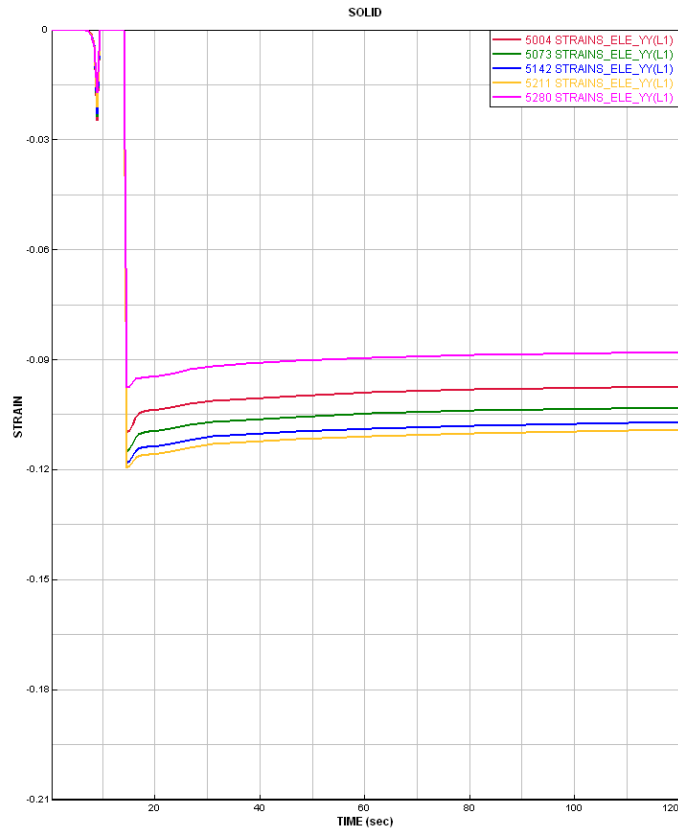


Figure 36. Continuous strain in elements marked with red in Figure 34.

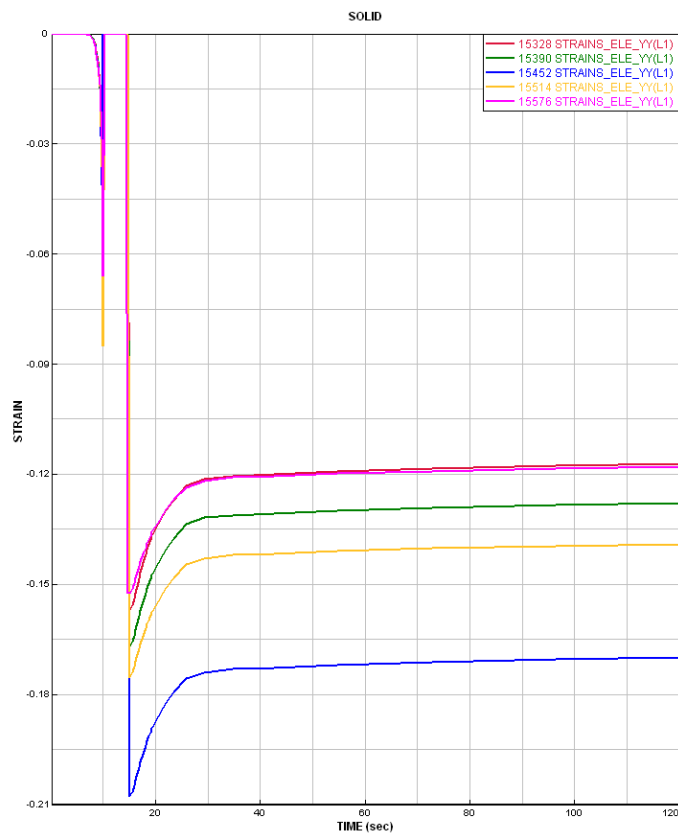


Figure 37. Continuous strain in elements marked with red in Figure 35.

When comparing the results from the simulations of the two specimens welded with half V-joint it can be seen that the strains are larger in the specimen with 2,5mm gap compared to the specimen with 0mm gap. It is not possible to draw any clear conclusions from these simulations since no cracks could be seen in the cross-sections of the two specimens. However, it is most likely that the specimen with the 2,5mm gap have a larger susceptibility to form hot cracks, compared to the specimen with 0mm gap. When comparing the two specimens prepared with half V-joint with land the same phenomenon can be seen. No significant differences in strain levels can be seen while comparing the two joint preparation types. However, since no cracks were detected in the cross-section analysis it is not possible to draw any conclusion regarding different crack susceptibility between the two preparations.

7 Spridning och publicering

7.1 Kunskaps- och resultatsspridning

Hur har/planeras projektresultatet att användas och spridas?	Markera med X	Kommentar
Öka kunskapen inom området	X	
Föras vidare till andra avancerade tekniska utvecklingsprojekt	X	A full project is planned
Föras vidare till produktutvecklingsprojekt	X	After finished full project
Introduceras på marknaden	X	After finished full project
Användas i utredningar/regelverk/ tillståndsärenden/ politiska beslut		

7.2 Publikationer

No external publications have been produced within the pre-study.

8 Discussion

The SEM-analysis of the cracks did show that the cracks originated from the solidification and hereby were hot cracks. The EDS- and WDS-analysis however did not show any significant signs of segregation. These results indicate that the occurrence of hot cracks is not only affected by the segregation of elements into the centreline of the welded material. However, since one issue with the analysis method is the overlapping of emitted energy for Molybdenum and Sulphur no clear conclusions regarding segregation can be drawn from these results.

The results from the 2D-simulations showed that this 2D-model was insufficient to predict the risk for hot-cracks. The insufficiency is thought to derive from the application of heat. The heat is applied instantaneously to the welded area in this model, which leads to a large temperature difference between the welded material and the base material, which in turn leads to large thermal strains in the solidification line. The use of a heat source, like in the 3D-simulations, would most likely reflect the actual process better. It is also thought that the heat conduction is not fully reflected in this model, since no conduction takes place along the weld.

The results from the 3D-simulations show a correlation between the strains during the solidification and the risk for hot cracks. The strains in focus are in the transversal direction of the crack, since large negative values of these strains are thought to open the crack and initiate propagation. As illustrated in chapter 6.3.2 large differences can be seen between specimens with a centreline hot crack and specimens free from cracks. These results indicate that the model can be used in order to compare different joint preparation with respect to hot crack susceptibility and hereby be used in order to optimize the welding process.

The cases described in chapter 6.3.3 were tested in order to evaluate the possibility to use the model for comparison of two other different joint preparations. However, the results from these tests do not show a

significant difference in crack-susceptibility between the two different preparations. It is however possible that these two cases have similar crack-susceptibility rates since no cracks were detected in the cross-section analysis of the welds. In order to fully evaluate the possibility to use the model for joint preparation optimization more tests needs to be performed, especially cases which are known to have different susceptibility for cracking.

It is shown that the model can compare the crack susceptibility between different cases as it is today. However, to get an increased industrial use of this method simulation of weld penetration is needed in order to enable fully virtual testing without the need of physical welding. It is also worth noticing that the model only can compare the crack susceptibility between different joints and not give an absolute answer regarding when cracking will occur.

It is also of interest to use the model for comparison of different material grades, both for base- and filler materials. In order to develop the model for this kind of testing further physical tests is needed together with investigation of high temperature properties for the different materials. Another interesting topic for further evaluation of the model is to simulate full sized real components; this would require further investigations of the impact of boundary conditions, both mechanical and thermal. In order to make the method more effective and save a lot of time consuming work further development of the post processing is needed, since the evaluation of the welds are considered to be highly time consuming at the moment.

9 Conclusions

The results from the study show a correlation between strains in the weld during solidification and the crack susceptibility in the welds. This correlation can be used in order to compare the risk for hot-cracks between different welds. It is thought that the model can be used in order to optimize weld preparations and processes, and to be used as a tool for analysis of crack susceptibility between different joints. However, it is not possible to use the model for prediction of cracks; it can only be used in order to compare different processes or joint preparations.

The model could possibly, with further development, be used as a tool for prediction of hot crack susceptibility in industrial cases. However, further development and evaluation is needed for implementation. In order to gain practical use of the model evaluation of full sized components needs to be performed. It would also be of interest to evaluate the model with respect to different material grades in order to use it as a tool for construction planning. A further development of the post processing is also needed in order to enable implementation in the industry.

10 Future work

In order to enable the model as a predictive tool in the industry further work is needed. It would be of interest to expand the test matrix in order to further verify the model. It would also be of interest to evaluate the possibility to use the model for comparison of different material grades, to test full sized components and to develop the post processing. An additional interesting topic would be to combine the model with simulations of weld penetration in order to digitalize the entire process planning, since the model used in this project requires physical testing for investigation of the weld penetration.

11 Deltagande parter och kontaktpersoner

ExTe	Per Olsson
Huddig	Mikael Danielsson
HIAB	Nikola Mrdjanov
HIAB	Eric Lindgren
HIAB	Niklas Rosendal
Voestalpine Böhler welding	Lars-Åke Bylund
Scania Ferruform	Mikael Juntti
ESAB	Peigang Li
ESAB	Maria Blixt
Swerea KIMAB	Paul Janiak
Swerea KIMAB	Joakim Wahlsten
Swerea KIMAB	David Löveborn
Swerea KIMAB	David Franklin

12 References

- [1] D. W. Walsh, M. L. Bright, T. L. Jackson, and D. B. Gibbs, "A Weldability Study of Nickel-Iron-Cobalt Hydrogen Resistant Alloys Using Weld Simulation in Parallel with Variable Restraint Testing," *Mater. Sci. Forum*, vol. 638–642, pp. 3763–3768, Jan. 2010.
- [2] J. C. Lippold, "Recent developments in weldability testing," *Hot Crack. Phenom. Welds*, pp. 271–290, 2005.
- [3] S. Kou, "Solidification and liquation cracking issues in welding," *Jom*, vol. 55, no. 6, pp. 37–42, 2003.
- [4] S. T. Mandziej, "Testing for Susceptibility to Hot Cracking on Gleeble™ Physical Simulator," *Hot Crack. Phenom. Welds*, pp. 347–376, 2005.
- [5] M. L. Gallagher, "AN INVESTIGATION OF THE ELEVATED TEMPERATURE CRACKING," *Thesis Dr.*, 2008.